Pergamon

Bioorganic & Medicinal Chemistry 7 (1999) 1163–1170

BIOORGANIC & MEDICINAL CHEMISTRY

Docking Experiments in the Flexible Non-nucleoside Inhibitor Binding Pocket of HIV-1 Reverse Transcriptase

Stephen J. Titmuss, Paul A. Keller* and Renate Griffith

Department of Chemistry, University of Wollongong, Northfields Ave, Wollongong, NSW 2522, Australia

Received 13 October 1998; revised 25 December 1998

Abstract—Docking experiments were undertaken using a number of published crystal structures of HIV-1 reverse transcriptase complexes with various non-nucleoside inhibitors. The docking method was validated by successfully docking each ligand, in the conformation found in the crystal structure of the complex with the enzyme, back into its binding pocket in the right orientation and position. Each ligand was then subjected to conformational searching and a database of unique low-energy conformations of all ligands established. Docking this database into each of the reverse transcriptase binding pockets showed that all inhibitors could be fitted into each different pocket, without alteration of the pocket geometry. This contradicts findings from earlier docking investigations and implies that the conformation of the binding pocket in each different complex is conserved sufficiently to allow particular uniform ligand binding modes. The inhibitor conformations selected by this docking process are mostly the same as the one the ligand adopts in its own pocket and the selected conformations and orientations exhibit an impressive degree of similarity in the arrangement of their steric and electronic features. A correlation has also been observed between inhibitor flexibility and tightness of fit into the pockets with the more flexible inhibitors achieving a tighter fit and thus fewer favourable orientations upon docking.

Introduction

Reverse transcriptase (RT) performs several critical roles in the replicative cycle of the human immunodeficiency virus (HIV), and thus considerable effort has been directed towards this enzyme as a target for therapies treating the acquired immune deficiency syndrome (AIDS). A striking feature of RT is its considerable conformational flexibility[1,2] (believed to be essential for several of its catalytic actions),[3] which has complicated attempts at traditional structure-based design of non-nucleoside RT inhibitors (NNRTIs).[4]

To date, fourteen crystal structures of HIV-1 RT in the apo form[1,5,6] and complexed with nine different non-nucleoside inhibitors have been published.[7–14] These structures have provided a great deal of insight into the conformational flexibility of RT, including the structural changes that are induced by binding of NNRTIs.

The crystal structures have shown that although portions of the inhibitor binding pocket (NNIBP) possess similar geometry in each of the NNRTI complexes, several regions undergo significant conformational changes when bound to different inhibitors. The volume of the pocket can differ by up to 100 Å^3 between the different complexes.[5,7,8,10] Despite this variability in NNIBP structure, the crystal structures show that the inhibitors, in their bound conformation, achieve a relatively good degree of steric overlap with one another. The compounds nevirapine, 1051U91, α-APA, HEPT and 9-Cl-TIBO (Fig. 1) occupy a common volume of 100 Å^3 out of a total volume of 440 Å^3.[8,10]

Docking studies involving non-nucleoside inhibitors and HIV reverse transcriptase have been performed previously,[4,15,16] and have shown that the differing pocket geometries can affect the validity of the relative ligand binding energies calculated when docking other NNRTIs into the cavity.[4] Most importantly, it has been shown that the optimal binding energy is most often obtained only when the correct NNIBP structure for each particular inhibitor is used as the starting conformation.[4] According to this study, the changes in NNIBP conformation serve to optimise, and 'customise', the protein–ligand interactions with each inhibitor.[4] The consequence of this customisation of pocket geometry is said to render ineffective the use of any 'consensus' NNIBP structure for accurate modelling of protein–ligand binding for anything but the most closely related NNRTI analogues.

Key words: Automated docking; enzyme-inhibitor complexes; non-nucleoside inhibitors; reverse transcriptase.
*Corresponding author. E-mail: paul_keller@uow.edu.au

0968-0896/99/$ - see front matter
PII: S0968-0896(99)00012-7

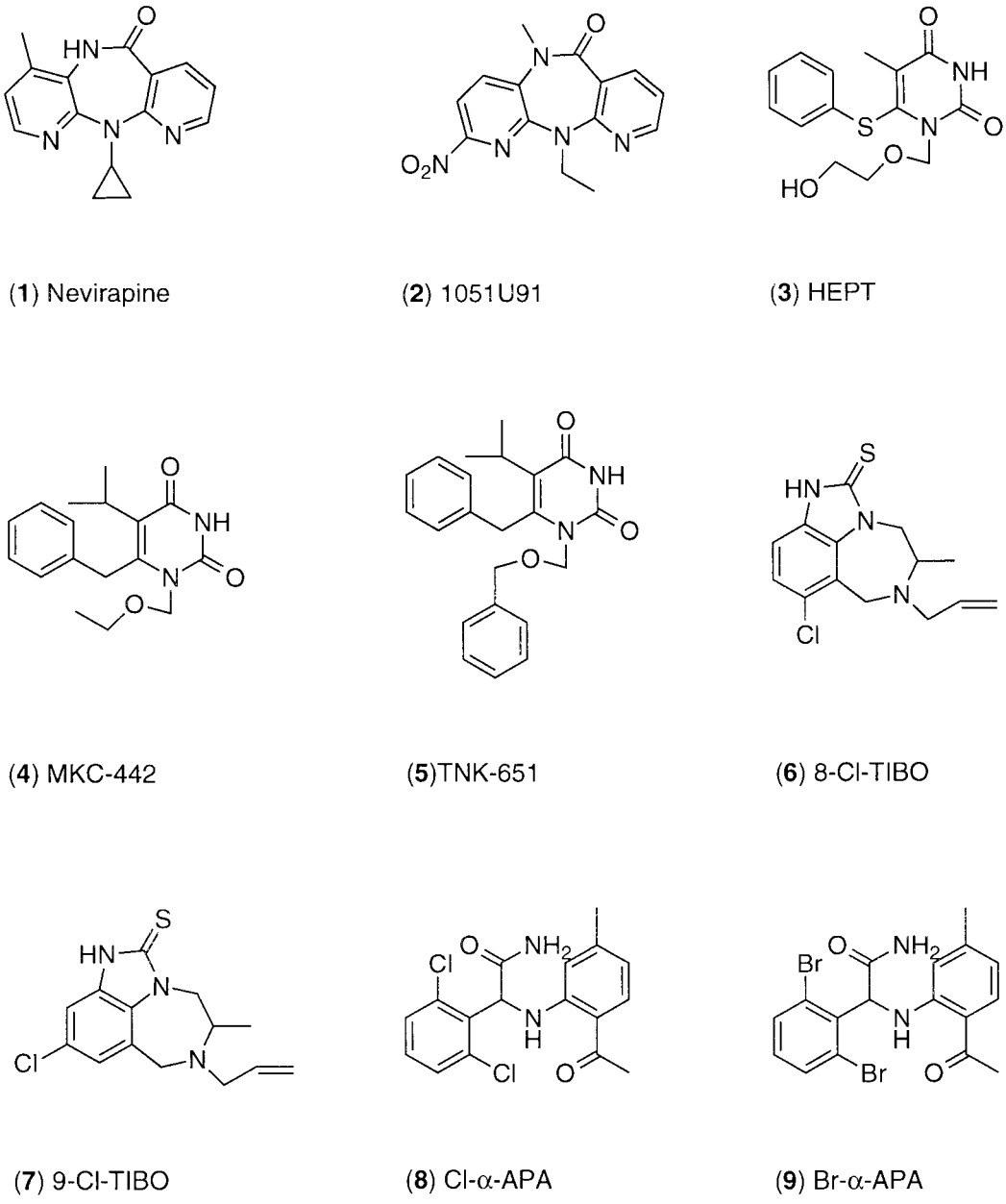

Figure 1. Non-nucleoside HIV-1 reverse transcriptase inhibitors used in this study.

Although these previous docking experiments allowed limited flexibility of the NNIBP amino acids and optimisation of the ligand conformation within the pocket, they have studied only a limited range of NNRTIs.

To investigate the effect of the NNIBP conformational changes on inhibitor binding, it was attempted to dock the various inhibitors into the different pocket geometries. The approach employed in our study was to generate a series of low energy conformations of many different inhibitors prior to docking into a larger range of different pocket geometries, using an automated molecular docking program. Although this method does not explicitely treat NNIBP flexibility, or account for the effect of protein–ligand interactions on the conformation of the inhibitor, it enables the binding potential for a large number of inhibitors and conformations to be determined relatively rapidly.

Results

Docking was performed on the seven high resolution crystal structures determined by Ren et al., complexed with the NNRTIs nevirapine (**1**),[10] 1051U91 (**2**),[10] HEPT (**3**),[10] MKC-442 (**4**),[7] TNK-651 (**5**),[7] Cl-α-APA (**8**)[10] and 9-Cl-TIBO (**7**).[8] These structures were selected because of their comparatively high resolution (2.2–3.0 Å) and uniform crystal space group. Use of structures within the same crystal packing prevents any structural changes introduced by different crystal lattice forces, rather than the binding of different inhibitors, complicating interpretation of the results. Inhibitors were,

however, selected from the entire set of available crystal structures (as their conformations were to be altered anyway), and include 8-Cl-TIBO (**6**) and Br-α-APA (**9**), in addition to those listed above. The chemical structures of the inhibitors are presented in Figure 1.

The program DOCK 3.5 (Department of Pharmaceutical Chemistry, University of California, San Francisco) was used in all docking experiments. DOCK explores many different relative alignments of ligand and receptor molecules, in order to determine geometrically and energetically feasible ligand binding modes.[17–24]

Validation of the docking method

To ensure that the ligand orientations and positions obtained from the docking studies were likely to represent valid and reasonable potential binding modes of the inhibitors, the DOCK program docking parameters and our sphere selections (see Experimental) had to first be validated for each crystal structure used. Each NNRTI, in the conformation found in the crystal structure of the RT-NNRTI complex, was docked into its corresponding binding pocket, to determine the ability of DOCK to reproduce the orientation and position of the inhibitor observed in the crystal structure.

Contact scoring calculations showed that in six of the seven crystal structures, on the basis of shape complementarity only, DOCK determined the optimal orientation of the docked inhibitors to be close to that of the original orientation found in the crystal (see Table 1). The low RMS deviations (all below 1 Å, for all heavy atoms) between the docked and crystal ligand coordinates indicate very good alignment of the experimental and calculated positions, especially considering the resolution limit of the crystal structures (2.2–3.0 Å). Visual inspection of the docked coordinates relative to the crystal structure NNRTI coordinates showed that in all cases the top three scoring results, and usually more, had orientations very similar to the crystal structures.

The high proportion of correct contact scored orientations calculated in each pocket indicates that the conformation of the NNIBP alone, contains enough information to accurately reproduce the crystal structure binding mode of the inhibitor, without requiring further π-stacking and electrostatic complementarity to distinguish them from other binding modes. This implies that the three-dimensional shapes of each pocket are highly mutually complementary with that of their respective NNRTIs.

Table 1. Docking of NNRTI crystal conformations

Inhibitor	PDB file	Contact		Forcefield	
		RMS	Orientations	RMS	Orientations
Nevirapine	1VRT	0.331	318	0.480	554
1051U91	1RTH	0.915	676	0.756	581
HEPT	1RTI	0.946	45	0.895	42
MKC-442	1RT1	0.679	3	0.613	13
TNK-651	1RT2	0.495	3	0.417	4
9-Cl-TIBO	1REV	—	0	—	0
Cl-α-APA	1VRU	0.980	70	0.786	53

Highest scoring orientations from docking of seven NNRTIs into their NNIBPs in the conformation found in their respective crystal complexes, using contact and forcefield scoring. RMS deviation of highest scoring orientation from that reported in the crystal structures, and the total number of ligand orientations found by DOCK for each scoring scheme. DOCK could find no favourable orientations of 9-Cl-TIBO in either scoring mode.

The exception was 9-Cl-TIBO, for which no orientations were docked into the binding pocket. This could possibly be due to particularly close association between the inhibitor and protein in the crystal structure, thus producing a large number of steric clashes and preventing any favourable calculated interactions. A contact scored docking run in which the size of the inhibitor was reduced, by removing all hydrogens from the ligand, returned 4394 favourable docked orientations, however, the highest scoring orientation had a RMS deviation of almost 2 Å from the crystal structure.

Similar results were obtained when using a force field scoring scheme for measuring protein–ligand interaction energies (see Table 1). The good correlation between the docked and crystal positions and orientations obtained, using contact and force field scoring was, however, not repeated when attempts were made to optimise the ligand positions using rigid body minimisation prior to scoring. Nevirapine, docked into its own NNIBP geometry had very large RMS deviations (>3 Å) for the highest scoring orientations and both the orientation and position of the ligand were completely different to the crystal structure. Since excellent reproduction of the crystal binding mode was achieved without rigid body minimisation, this method was not pursued any further.

As none of the structural waters are conserved amongst all the RT-NNRTI crystal complexes, the docking experiments were performed without water molecules in the NNIBPs. To test this procedure, nevirapine was docked into the binding pocket in the presence of the single water molecule located within the pocket in the crystal structure. The ten best scoring results were all in identical relative positions to those calculated in the absence of water.

Docking of multiple ligand conformations

Multiple low energy conformations of each inhibitor were generated using a simple molecular dynamics (100 fs at 900 K, followed by collection of 50 conformations, each after 1 ps at 900 K) and minimisation protocol and a unique set of conformations was collected by selecting a set of conformations that differed by at least 0.3 Å RMS from each other. The selected conformations covered the range of energies of the entire set from the molecular dynamics calculations. The conformation of the ligand in the crystal structure was added to the set.

The number of unique conformations generated for each ligand varied enormously (Table 2), and gives some perception of the flexibility of the different NNRTIs.

Table 2. Unique conformations of NNRTIs

Inhibitor	Compound No.	Conformations	Energy range (kcal mol^{-1})	RMS range (Å)[c]
Nevirapine	(**1**)	2	142.2–142.2	0.6–1.4
1051U91[a]	(**2**)	6	61.7–74.0	0.3–2.0
HEPT	(**3**)	29	3.6–9.5	0.3–2.2
MKC-442	(**4**)	20	3.7–10.3	0.3–1.7
TNK-651	(**5**)	38	9.1–14.2	0.5–2.9
8-Cl-TIBO	(**6**)	20	24.0–29.4	0.7–2.5
9-Cl-TIBO	(**7**)	22	22.6–28.1	0.8–2.7
Cl–α-APA	(**8**)	7	6.1–13.8	0.6–2.1
Br-α-APA[b]	(**9**)	12	7.7–15.2	0.9–2.7

[a]Nitro substituent replaced by carboxylate, see Experimental.
[b]Dibrominated analogue of Cl-α-APA.
[c]All heavy atoms were used for superimposition.
Number of conformations of each NNRTI differing by at least 0.3 Å RMS after molecular dynamics and minimisation, ranges of minimised energies and RMS deviations from the conformation of the ligand in its complex with RT of the selected conformations.

It was expected that the specific geometry of each pocket would provide some filtering of the large set of structures used as input for DOCK to yield a relatively small and characteristic set of compounds and conformations, that would allow the interpretation of the ligand and NNIBP conformational features that gave rise to the binding mode of each docked compound.

When contact scoring was employed, DOCK was, however, much more prolific in its ability to dock the input structures into the pockets than anticipated. Between 66 and 99% of the database was successfully docked into all NNIBP structures.

Application of force field scoring to the database proved to be more promising, reducing the number of docked conformations significantly, and these docking results are the ones interpreted in the next sections.

Inspection of the 10 to 20 highest scoring inhibitor conformations, and their relative orientations, after docking and forcefield scoring of the database, showed only limited specificity for the inhibitor from which the NNIBP structure was derived. Conformations of nevirapine and 1051U91 dominated the highest scoring structures of most of the seven binding pocket geometries, despite the protein structure being derived from a different NNRTI complex. In four cases, the highest scoring conformation did not even belong to the original ligand in the complex from which the structure was derived (Table 3). This suggests that, despite the difference in pocket shape, only relatively minor adjustments of each ligand conformation are required to allow the NNRTIs to fit into other pockets. Reassuringly, the highest scoring conformation of nevirapine, MKC-442, Cl-α-APA, TNK-651 and 1051U91, when docked into their own pocket, was found to be identical or very similar to the conformation in the crystal structure of the complex. For HEPT the RMS value between the docked conformation and the one in the crystal structure was also not very large (0.351). The 1REV pocket again was the only one where the original ligand 9-Cl-TIBO (**7**) was not docked in amongst the 15 highest scoring structures.

While the docking scores are, strictly speaking, not directly comparable for different ligands in different pockets, the scores for one ligand in different pockets should at least be similar and this was indeed found to be the case for nevirapine (**1**) (Table 4). As mentioned above, nevirapine fits into all pockets (except for the 1RTH pocket) very well as evidenced by the high rank of the highest scoring nevirapine conformation.

Superposition of the docked conformations over the crystal structure orientation of the original inhibitor of each pocket showed very good alignment of major structural features. Despite the structural diversity of the NNRTIs, the aromatic rings of most of the high scoring docked conformations were aligned with one another and with the crystal structure orientation, as were many of the various other functional groups in the inhibitors. This suggests that a significant contribution to the docking scores was made by the electrostatic component of π-stacking interactions between the inhibitors and NNIBPs. Those conformations that had large rotations relative to the majority of the other docked conformations still retained a good degree of overall steric overlap, occupying the same volume even if the correspondence between functional groups was not conserved.

Figure 2 shows the high degree of steric similarity and overlap of the conformations docked into a NNIBP structure of each of the four classes of NNRTI examined. Each component of Figure 2 shows the crystal structure conformation of the inhibitor from which the pocket structure was derived, and five different NNRTIs in their highest scoring conformation and relative orientation, from two different view points. A significant

Table 3. Docking of the ligand database into the different pockets

Highest scoring inhibitor (forcefield scoring) docked into each pocket				
Pocket[a]	Inhibitor in crystal structure	Inhibitor docked	Score	Comments
1VRT	Nevirapine (**1**)	1051U91 (**2**)	−36.334	(**1**) ranked 3rd, score very close, RMS[b] 0.00
1RT1	MKC-442 (**4**)	TNK-651 (**5**)	−40.321	(**4**) ranked 2nd, RMS[b] 0.00
1VRU	Cl-α-APA (**8**)	Cl-α-APA (**8**)	−41.277	RMS[b] 0.00
1REV	9-Cl-TIBO (**7**)	1051U91 (**2**)	−33.967	(**7**) not in first 15 structures
1RT2	TNK-651 (**5**)	TNK-651 (**5**)	−46.946	RMS[b] 0.00
1RTH	1051U91 (**2**)	1051U91 (**2**)	−37.662	RMS[b] 0.06
1RTI	HEPT (**3**)	MKC-442 (**4**)	−31.330	(**3**) ranked 4th, RMS[b] 0.35

[a]See Table 5 for codes.
[b]Superimposition of all heavy atoms with crystal conformation (see text).

Table 4. Docking of nevirapine (**1**) into the different pockets

Highest scoring conformation (forcefield scoring) of nevirapine docked into each pocket

Pocket[a]	Inhibitor in crystal structure	Score	Rank	RMS[b]
1VRT	Nevirapine (**1**)	−35.687	3	0.00
1RT1	MKC-442 (**4**)	−31.369	4	0.59
1VRU	Cl-α-APA (**8**)	−34.815	3	0.00
1REV	9-Cl-TIBO (**7**)	−32.238	2	1.37
1RT2	TNK-651 (**5**)	−30.042	3	0.00
1RTH	1051U91 (**2**)	−32.599	14	0.00
1RTI	HEPT (**3**)	−33.997	2	0.00

[a]See Table 5 for codes.
[b]Superimposition of all heavy atoms with crystal conformation.

feature of the superposed structures is the alignment of the butterfly-like curvature of each NNRTI, as shown in the left hand column of Figure 2, amongst the various types of inhibitor structure. The 9-Cl-TIBO NNIBP possessed the least degree of complementarity in the overlayed docked structures, and the original inhibitor itself was not amongst the first five different inhibitors docked into the pocket.

Discussion

The docking study of Kroeger Smith et al.[4] found that a reliable correlation between the calculated binding

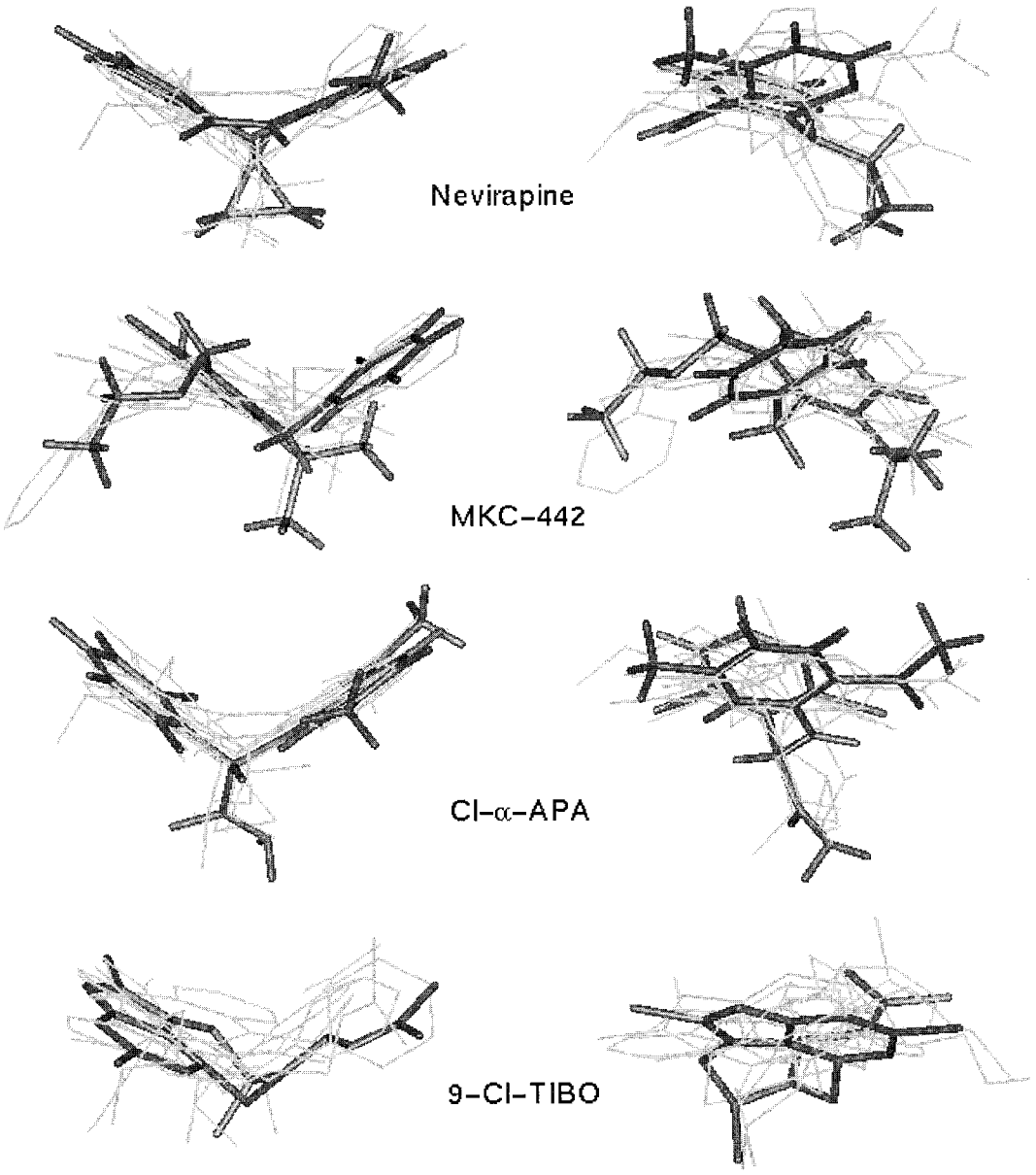

Figure 2. Shape complementarity of Docked NNRTIs. Relative orientation of the highest scoring conformation of each of the five highest ranking structures (thin lines) docked into the NNIBPs of the named inhibitors (crystal structure conformation drawn in thick lines). Two different perspectives are shown of each overlay (left and right columns, respectively).

energy and experimental inhibitory potency could not be made when an inhibitor was docked into a NNIBP geometry not derived from its own crystal complex. While the current study has not determined binding energies, it has been demonstrated that the five docked ligands shown in Figure 2, drawn in grey, belong to at least three of the four different classes of NNRTI in each case, suggesting that with reasonable adjustments of conformation, most NNRTIs are capable of fitting into the different NNIBP geometries. The ability of DOCK to fit low energy conformations of different NNRTIs into the one pocket geometry, often with better scores than conformations of the original ligand, implies that the NNIBP shape may not have as great an influence on docking calculations as previously suggested. DOCK orients ligands on the basis of steric factors only, therefore these results show that the pocket geometry is sufficiently similar in the different complexes to allow other NNRTIs to fit into the cavity. Although the NNIBP has been reported to change conformation and volume with different NNRTIs, the steric and chemical complementarity illustrated in Figure 2 suggests that a considerable amount of structural similarity remains, particularly the features that favour the butterfly shape and aromatic character of inhibitors.

There is a correlation between inhibitor flexibility and the number of docked orientations calculated. The more rigid ligands, nevirapine and 1051U91, can fit into the binding site with several hundred favourable orientations, while the flexible NNRTIs, such as HEPT and analogues, can adopt comparatively fewer favourable orientations. This suggests that the association between ligand and pocket may be closer for the more flexible molecules. This could be so because the combined conformational freedom in both the binding pocket and the inhibitor may allow both to adopt a more mutually complementary geometry, leaving minimal "free space" in the cavity to allow the ligand to adopt other orientations during docking whereas the rigid NNRTIs must rely almost entirely upon conformational change of the NNIBP to tailor the interaction.

Calculation of the proportion of each NNIBP geometry filled by its ligand, from the reported pocket and inhibitor volumes[7,8,10] provides some support for this. Flexible HEPT derivatives occupy around 45% of the NNIBP, whereas the rigid ligands occupy around 36%.

This could also explain the inability of DOCK to fit the 9-Cl-TIBO back into its own binding pocket. The flexibility of this ligand may allow a particularly close fit with its binding site, producing steric interactions during docking that were above the acceptable limits of the program parameters.

In most cases, the highest scoring conformation of any ligand docked into any pocket is the same conformation that the ligand adopts in the crystal structure of its complex with RT. This preference for the docking of crystal conformations may be related to the fact that the conformational searching was performed in vacuo, while the crystal conformations are in a protein environment and so may be better suited to interacting with the general pocket environment.

Conclusion

A validated docking study on a set of unique conformations of nine non-nucleoside inhibitors into the empty binding pockets of seven different reverse transcriptase–inhibitor complex crystal structures has been undertaken. Four major findings have been discussed in this paper. Firstly, all inhibitors could be fitted into all binding pockets, without alteration of the pocket geometries. The inhibitor conformations and orientations selected by the automated docking program exhibit a large degree of similarity in the arrangement of steric features and aromatic rings and the crystal conformation of the ligand is usually preferred, even when the ligand is docked into a different pocket. Lastly, a correlation has been observed between inhibitor flexibility and the number of docked orientations calculated with the more flexible inhibitors achieving a tighter fit and thus fewer favourable orientations in the pocket

Experimental

Atomic coordinates for all three dimensional protein models were obtained from the Brookhaven Protein Data Bank.[25,26] A total of 14 sets of high resolution crystal structures of HIV-1 RT in NNRTI complexes or apo form were downloaded. Table 5 lists the crystal structures (not all were used in this work) and some statistics relevant to the accuracy of the coordinates.

Docking studies were performed using DOCK version 3.5 (Department of Pharmaceutical Chemistry, University of California, San Francisco).[27] The FORTRAN 77 source code supplied was compiled and used without further modification, as were all utility and script programs (except for utility program autoMS, where a minor error was detected; details available from the authors upon request).

Crystal structure preparation and sphere generation

Ligands and all crystallographic waters were removed from the atomic coordinate data files and hydrogens added to the protein. As some DOCK utility programs cannot work with the extremely large RT coordinate sets, a reduced subset of the structure was used for processing by selecting only thoses residues lying within 25 Å of the C_α atom of p66 Tyr188. The NNRTI binding region was defined by selecting a further subset of residues within 10 Å of the location of the inhibitor in the crystal structure. The solvent accessible surface of this 10 Å subset was generated at a density of three surface points per $Å^2$ using the MS program with a 1.4 Å probe.[20,21] Spheres with radii between 1.4 and 4.0 Å filling potential binding pockets on the solvent accessible surface were generated using the DOCK utility SPHGEN, grouped into clusters of overlapping spheres and manually edited to remove those that did not fall

Table 5. Details of RT X-ray crystal structures

PDB Code	Inhibitor	Resolution	*R*-Factor	Space group	References
1REV	9-Cl-TIBO	2.6 Å	0.224	$P2_12_12_1$	8
1RT1	MKC-442	2.55 Å	0.197	$P2_12_12_1$	7
1RT2	TNK-651	2.55 Å	0.207	$P2_12_12_1$	7
1RTH	1051U91	2.2 Å	0.214	$P2_12_12_1$	10
1RTI	HEPT	3.0 Å	0.236	$P2_12_12_1$	10
1RTJ	None	2.3 Å	0.219	$P2_12_12_1$	10,5
1VRT	Nevirapine	2.2 Å	0.186	$P2_12_12_1$	10
1VRU	Cl-α-APA	2.4 Å	0.187	$P2_12_12_1$	10
1DLO	None	2.7 Å	0.249	*C*2	1
1TVR	9-Cl-TIBO	3.0 Å	0.259	*C*2	13
1UWB	8-Cl-TIBO	3.2 Å	0.274	*C*2	13
1HMV	None	3.2 Å	0.254	*C*2	6
1HNI	Br-α-APA	2.8 Å	0.255	*C*2	14
1HNV	8-Cl-TIBO	3.0 Å	0.249	*C*2	13,9
3HVT	Nevirapine	2.9 Å		C_2	11,9
1HMI	None	3.0 Å		$P3_212$	11,12

inside or around the entrance to the NNIBP, as determined by visual inspection, using InsightII version 95.0 (Molecular Simulations, Inc., San Diego). A short script was written to convert DOCK file formats into a format readable by InsightII. Generally, of the 150–240 spheres generated for each crystal structure, approximately 60–70 were sufficient to describe the NNIBP.

Contact and forcefield scoring grid preparation

The grids for docking were generated at a density of three grid points per Å for the region enclosing the spheres with an extra margin of three Å. Contact grids were calculated by distmap with receptor hydrogen atoms removed, close contact limits for polar and non-polar atoms of 2.3 and 2.8 Å, respectively, and a cutoff distance of 4.5 Å. Forcefield scoring grids, generated by chemgrid, were calculated using AMBER[28,29] parameters and the receptor structure with hydrogen atoms added, a distance dependent dielectric function of $4.5r$, polar and carbon atom close contact limits of 2.3 and 2.8 Å, respectively, and a nonbonded interaction cutoff of 10 Å.

Ligand preparation

After extraction of ligand atom coordinates from the RT/inhibitor complex struture PDB files, hydrogen atoms were added, bond orders corrected and CFF91 force field potentials set using InsightII. For 1051U91, the ligand in the PDB file 1rth was different to the structure reported in the literature[10] and was corrected. There are no parameters for the nitro substituent on the pyridine ring of 1051U91 in either the CFF91 or the CVFF force fields and this had to be replaced by a suitable group. The carboxylate group was selected.

Inhibitor conformations were generated using the CFF91 force field and Discover version 2.9.7 (MSI, San Diego, USA) via InsightII. The molecular dynamics and minimisation protocol for the conformational searching involved initialisation of dynamics at 900 K for 100 fs, followed by 50 consecutive dynamics runs at 900 K for 1 ps each. The 50 conformations were then minimised for 100 iterations using steepest descents and then with conjugate gradients until the maximum derivative was less than 0.0001 kcal $Å^{-1}$. Cluster graph analysis in InsightII of each set of dynamics conformations revealed many duplicate or very similar conformations (RMS values within 0.3 Å), which were subsequently discarded from the data set. This left between 2 (Nevirapine) and 38 (TNK-651) 'unique' conformations (17 on average for the 9 inhibitors). The resulting 156 conformations were combined with the original crystal conformation of each of the ligands into a DOCK 3.5 format database using DOCK utilities.

Ligand docking and database searching

Ligand docking was performed using both force field (AMBER parameters) and contact (van der Waals only) scoring options. The chemical matching, degeneracy checking, critical sphere clustering and ligand mirroring options of DOCK 3.5 were not used. The default DOCK 3.5 parameters were used for all options unless otherwise specified. The output from each dock run was sorted according to contact or force field score, as appropriate, and a set of the best 5–20 conformations/orientations extracted using DOCK utilities. Visual inspection of relative positions required superposition of the crystal structure and docked inhibitor coordinates using Insight II. A UNIX script was written for the rapid extraction of contact, force field and RMS scores from DOCK output files.

Acknowledgements

The authors wish to thank Ms. Tien Luu from the Department of Chemistry, University of Wollongong, for her help with the interpretation of the reverse transcriptase complex structures.

References

1. Hsiou, Y.; Ding, J.; Das, K.; Clark Jr., A. D.; Hughes, S. H.; Arnold, E. *Structure*, **1996**, *4*, 853.
2. Jäger, J.; Smerdon, S. J.; Wang, J.; Boisvert, D. C.; Steitz, T. A. *Structure*, **1994**, *2*, 869.

3. Patel, P. H.; Jacobo-Molina, A.; Ding, J.; Tantillo, C.; Clark Jr., A. D.; Raag, R.; Nanni, R. G.; Hughes, S. H.; Arnold, E. *Biochemistry* **1995**, *34*, 5351.
4. Kroeger Smith, M. B.; Rouzer, C. A.; Taneyhill, L. A.; Smith, N. A.; Hughes, S. H.; Boyer, P. L.; Janssen, P. A. J.; Moereels, H.; Koymans, L.; Arnold, E.; Ding, J.; Das, K.; Zhang, W.; Michejda, C. J.; Smith Jr., R. H. *Prot. Sci.* **1995**, *4*, 2203.
5. Esnouf, R.; Ren, J.; Ross, C.; Jones, Y.; Stammers, D.; Stuart, D. *Nature Struct. Biol.* **1995**, *2*, 303.
6. Rodgers, D. W.; Gamblin, S. J.; Harris, B. A.; Ray, S.; Culp, J. S.; Hellmig, B.; Woolf, D. J.; Debouck, C.; Harrison, S. C. *Proc. Natl. Acad. Sci. USA* **1995**, *92*, 1222.
7. Hopkins, A. L.; Ren, J.; Esnouf, R. M.; Willcox, B. E.; Jones, E. Y.; Ross, C.; Miyasaka, T.; Walker, R. T.; Tanaka, H.; Stammers, D. K.; Stuart, D. I. *J. Med. Chem.* **1996**, *39*, 1589.
8. Ren, J.; Esnouf, R.; Hopkins, A.; Ross, C.; Jones, Y.; Stammers, D.; Stuart, D. *Structure* **1995**, *3*, 915.
9. Ding, J.; Das, K.; Moereels, H.; Koymans, L.; Andries, K.; Janssen, P. A. J.; Hughes, S. H.; Arnold, E. *Nature Struct. Biol.* **1995**, *2*, 407.
10. Ren, J.; Esnouf, R.; Garman, E.; Somers, D.; Ross, C.; Kirby, I.; Keeling, J.; Darby, G.; Jones, Y.; Stuart, D.; Stammers, D. *Nature Struct. Biol.* **1995**, *2*, 293.
11. Kohlstaedt, L. A.; Wang, J.; Friedman, J. M.; Rice, P. A.; Steitz, T. A. *Science* **1992**, *256*, 1783.
12. Smerdon, S. J.; Jäger, J.; Wang, J.; Kohlstaedt, L. A.; Chirino, A. J.; Friedman, J. M.; Rice, P. A.; Steitz, T. A. *Proc. Natl. Acad. Sci. USA* **1994**, *91*, 3911.
13. Das, K.; Ding, J.; Hsiou, Y.; Clark Jr., A. D.; Moereels, H.; Koymans, L.; Andries, K.; Pauwels, R.; Janssen, P. A. J.; Boyer, P. L.; Clark, P.; Smith Jr., R. H.; Kroeger Smith, M. B.; Michejda, C. J.; Hughes, S. H.; Arnold, E. *J. Mol. Biol.* **1996**, *264*, 1085.
14. Ding, J.; Das, K.; Tantillo, C.; Zhang, W.; Clark Jr., A. D.; Jessen, S.; Lu, X.; Hsiou, Y.; Jacobo-Molina, A.; Andries, K.; Pauwels, R.; Moereels, H.; Koymans, L.; Janssen, P. A. J.; Smith Jr., R. H., Kroeger Koepke, M.; Michejda, C. J.; Hughes, S. H.; Arnold, E. *Structure* **1995**, *3*, 365.
15. Luu, T. T. T. B.Med.Chem.(Hons) thesis, University of Wollongong, 1996.
16. Esnouf, R. M.; Stuart, D. I.; De Clercq, E.; Schwartz, E.; Balzarini, J. *Biochem. Biophys. Res. Comm.* **1997**, *234*, 458.
17. Kuntz, I. D.; Blaney, J. M.; Oatley, S. J.; Langridge, R.; Ferrin, T. E. *J. Mol. Biol.* **1982**, *161*, 269.
18. Meng, E. C.; Shoichet, B. K.; Kuntz, I. D. J. *Comp. Chem.* **1992**, *13*, 505.
19. DesJarlais, R. L.; Sheridan, R. P.; Seibel, G. L.; Dixon, J. S.; Kuntz, I. D.; Venkataraghavan, R. *J. Med. Chem.* **1988**, *31*, 722.
20. Connolly, M. L. *Science* **1983**, *221*, 709.
21. Connolly, M. L. *J. Appl. Cryst.* **1983**, *16*, 548.
22. Shoichet, B. K.; Bodian, D. L.; Kuntz, I. D. *J. Comp. Chem.* **1992**, *13*, 380.
23. Shoichet, B. K.; Kuntz, I. D. *Protein Eng.* **1993**, *6*, 723.
24. Meng, E. C.; Gschwend, D. A.; Blaney, J. M.; Kuntz, I. D. *Proteins Struct. Funct. Genet.* **1993**, *17*, 266.
25. Bernstein, F. C.; Koetzle, T. F.; Williams, G. J. B.; Meyer Jr., E. F.; Brice, M. D.; Rodgers, J. R.; Kennard, O.; Shimanouchi, T.; Tasumi, M. *J. Mol. Biol.* **1977**, *112*, 535.
26. Brookhaven Protein Data Bank. http://pdb.bnl.gov/.
27. Gschwend, D. A. (Ed.) DOCK Version 3.5 (February 1995) User Manual. Department of Pharmaceutical Chemistry, University of California, San Francisco, 1995.
28. Weiner, S. J.; Kollman, P. A.; Case, D. A.; Singh, U. C.; Ghio, C.; Alagona, G.; Profeta Jr., S.; Weiner, P. *J. Am. Chem. Soc.* **1984**, *106*, 765.
29. Weiner, S. J.; Kollman, P. A.; Nguyen, D. T.; Case, D. A. *J. Comp. Chem.* **1986**, *7*, 230.